Journal of Hazardous Materials 160 (2008) 295–300

Contents lists available at ScienceDirect

Journal of Hazardous Materials

journal homepage: www.elsevier.com/locate/jhazmat

Magnetically separable composite photocatalyst with enhanced photocatalytic activity

Yanhui Ao[a,b,c], Jingjing Xu[a,b,c], Xunwei Shen[b], Degang Fu[a,b,c,*], Chunwei Yuan[b]

[a] School of Chemistry and Chemical Engineering, Southeast University, Nanjing 210096, China
[b] State Key Laboratory of Bioelectronics, Southeast University, Nanjing 210096, China
[c] Key Laboratory of Environmental and Bio- Safety in Suzhou, Research Intitute of Southeast University, Dushu Lake Hogher Education Town, Suzhou 215123, China

ARTICLE INFO

Article history:
Received 8 November 2007
Received in revised form 28 February 2008
Accepted 28 February 2008
Available online 8 March 2008

Keywords:
Magnetic activated carbon
Magnetically separable
Photocatalysis
Titania
Phenol

ABSTRACT

A novel magnetically separable composite photocatalyst, anatase titania-coated magnetic activated carbon (TMAC), was prepared in this article. In the synthesis, magnetic activated carbon (MAC) was firstly obtained by adsorbing magnetic Fe_3O_4 nanoparticles onto the activated carbon (AC), and then the obtained MAC was directly coated by anatase titania nanoparticles prepared at low temperature (i.e. 75 °C). The prepared samples were characterized by XRD, SEM and vibrating sample magnetometer (VSM). The composite photocatalyst can be easily separated from solution by a magnet, its photocatalytic activity in degradation of phenol in aqueous solution also has dramatic enhancement compared to that of the neat titania.

1. Introduction

In recent two decades, heterogeneous photocatalysis has emerged as an efficient technology to decontaminate either wastewater or polluted air [1–3]. Several review articles have cited the theory of this technology which is based on the use of UV irradiated semiconductors, generally titania, to destroy various organic pollutants [4–6].

Photocatalytic activity of titania strongly depends on its microstructure and physical properties. A way to increase titania photocatalytic activity is the preparation of a nano-structural titania to get a high surface area which is directly related with photocatalytic activity of titania [4]. Typically, costly problems hinder their application in industry. When the small titania powder photocatalyst are applied as suspensions, it associated with catalyst leaching, settling and the need for eventual catalyst separation by filtration during treatment. Therefore, catalyst immobilization related research has attracted wide attention. Research had been carried out by immobilizing titania onto various substrates such as glass beads, sand, glass fiber in the form of mesh, or on reactor wall [7]. Although this approach provided a solution to the solid–liquid separation problem, slurry-type reactors offer significant advantages over immobilized-catalyst-type reactors in terms of the catalyst surface availability and superior mass-transfer properties [8].

Matos et al. [9] investigated the photocatalytic activity of a suspended mixture of titania and activated carbon. They found that there were a synergistic effect and a common interface, which contributed to the higher photocatalytic activity, between titania and activated carbon. Several other authors investigated the photocatalytic degradation of aqueous organic pollutants by titania-coated activated carbon in slurry-type reactors [10–12]. They also found enhanced photocatalytic activity of the composite photocatalyst. The separation problem still existed because the catalyst was size in micron grade, although it can be separated more easily than the slurry titania system.

To solve the problem in slurry photocatalytic reactor, some other authors prepared nanoparticles with magnetic core and photocatalytic titania shell [13–15]. The magnetic cores have been used including magnetite, maghemite nickel ferrite, etc. Although these catalysts could be separated easily by magnet, their photocatalytic activities were declined compared to that of neat titania. More recently, Misra and co-workers [16–19] prepared titania coated nickel ferrite, they found the composite photocatalyst can be applied as a removable anti-microbial photocatalyst and can be

* Corresponding author at: School of Chemistry and Chemical Engineering, Southeast University, Nanjing 210096, China. Tel.: +86 25 83793091; fax: +86 25 83793091.
E-mail addresses: andyao@seu.edu.cn, fudegang@seu.edu.cn (D. Fu).

0304-3894/$ – see front matter © 2008 Elsevier B.V. All rights reserved.
doi:10.1016/j.jhazmat.2008.02.114

extracted from the sprayed surface (human body or environment) after treatment. So the combination of magnetic nanoparticles with titania is very important for the practical application of titania photocatalysis technology.

In order to prepare a novel composite photocatalyst with enhanced photocatalytic activity, we combined the adsorption activity of activated carbon with the magnetic separability of Fe_3O_4 and photocatalytic activity of titania. In the present work, magnetic activated carbon (MAC) were prepared firstly by dispersing powder activated carbon in Fe_3O_4 sol which prepared by the co-precipitation of iron(II) and iron(III) in the presence of ammonium hydroxide. Then the titania, which prepared at low temperature, was deposited onto the MAC. At last, the photocatalyst thus prepared were applied to degrade phenol in aqueous solution. The photocatalytic activity was compared with three other catalysts, i.e. Degussa P25 titania, titania-coated activated carbon (TAC) and neat titania (NT) synthesized by the same method. Results show that the titania-coated magnetic activated carbon (TMAC) exhibited highest activity during photocatalytic degradation of phenol. Furthermore, it can be separated more easily from solution compared with other photocatalysts.

2. Experimental

2.1. Material and chemical

Activated carbon (AC) with specific surface area around 1100 $m^2\,g^{-1}$ was purchased from ShangHai Activated Carbon Ltd. $FeSO_4$ and $Ti(OBu)_4$ used in the experiment were chemical reagent grade. Nitric acid (HNO_3), isopropanol (PrOH) and $FeCl_3$ were analytical reagent grade. Distilled water was further cleaned prior to its use with a quartz sub-boil high purity water purification system.

2.2. Equipments

The dried samples (Fe_3O_4, Fe_3O_4/AC, Fe_3O_4/AC/TiO_2 powder) were analyzed for their magnetic properties, composition and microstructure. The magnetic measurements were carried out with a vibrating sample magnetometer (VSM, PARR, Model 4500). The structure properties were determined by X-ray diffractometer (XD-3A, Shimadazu Corporation, Japan) using graphite monochromatic copper radiation (Cu Kα) at 40 kV, 30 mA over the 2θ range 20–80°. The morphologies were characterized with a transmission electron microscopy (TEM, JEM2000EX). BET surface area measurements were carried out by N_2 adsorption at 77 K using an ASAP2020 instrument. The total pore volume was calculated from the amount of nitrogen adsorbed at relative pressure of 0.975. The HPLC system was Agilent 1100 with tunable absorbance detector adjusted at 270 nm for the detection of phenol. A reverse-phase column (length, 250 mm; internal diameter, 4.6 mm) Agilent Eclipse XDB-C18 was used. The mobile phase was composed of acetonitrile and deionized doubly distilled water. The v/v ratio CH_3CN/H_2O was 20/80 and the flow rate was 1 ml min^{-1}.

2.3. Catalysts preparation

Magnetic magnetite particles were prepared by chemical co-precipitation method as the following procedure: definite amount of $FeSO_4$ and $FeCl_3$ were dissolved in distilled water which was bubbled with N_2, the molar ratio of Fe^{3+} and Fe^{2+} was 5:3. Then, definite NH_4OH was added drop-wise into the solution at vigorous stirring till the pH 9. Finally, black magnetite sol was obtained.

MAC was prepared in the following way: 3 g of AC powder, which washed for three times by distilled water, was added into 200 ml of diluted Fe_3O_4 sol. Then the admixture was stirred for 1 h before kept at vacuum for 30 min. The solid phase of MAC was separated by a magnet and then dried at 40 °C.

For preparation of TiO_2 sol, $Ti(OBu)_4$ was chosen as a Ti precursor, which is less reactive than titanium chloride and titanium isopropoxide. 25 ml $Ti(OBu)_4$ diluted with 8 ml PrOH was added drop-wise into 200 ml distilled water under vigorous stirring, whose acidity was adjusted with HNO_3 to be pH 2.5. Then, the solution was kept under reflux condition (around 75 °C) for 24 h. Finally, pure TiO_2 sol was obtained after PrOH and *n*-butyl alcohol were removed from the solution in a rotatory evaporator under vacuum.

To obtain TMAC, the coating procedure of titania onto MAC was as following: 3 g of MAC was dispersed in titania sols in an ultrasonic bath for 1 h. Then, it was dried into powders in a rotatory evaporator under vacuum at 75 °C. The carbon content in the resultant composite photocatalysts was determined from the ignition loss at 700 °C in a flow of air.

2.4. Photocatalytic experimental

The photocatalytic activity of the prepared TMAC was assessed by degrading model contaminated water of phenol aqueous solution. The photocatalytic reaction system includes a photoreactor with a UV illumination source (18 W UV lamp with a wavelength peak at 365 nm). In a typical photocatalytic test performed at room temperature, 0.6 g prepared composite photocatalyst was added into 400 ml phenol solution. The concentration of phenol in solution was 100 mg L^{-1}. After kept in the dark under stirring for 1 h to reach adsorption equilibrium, the UV illumination started and 5 ml suspension were removed at regular intervals of 1 h for analysis.

2.5. Separation of TMAC

The process of separating photocatalyst can be illustrated by Scheme 1. In a demonstration experiment, the prepared photocatalyst was dispersed into aqueous solution by ultrasonic vibrating for 15 min. A magnet was applied to attract the magnetic photocatalyst onto the bottom. The solution was poured out without losing any catalyst. For a suspension of magnetic photocatalyst whose concentration was 1.5 g L^{-1}, the photocatalyst can be precipitated thoroughly in 4 min by a magnet of 1 T. The results show that the pho-

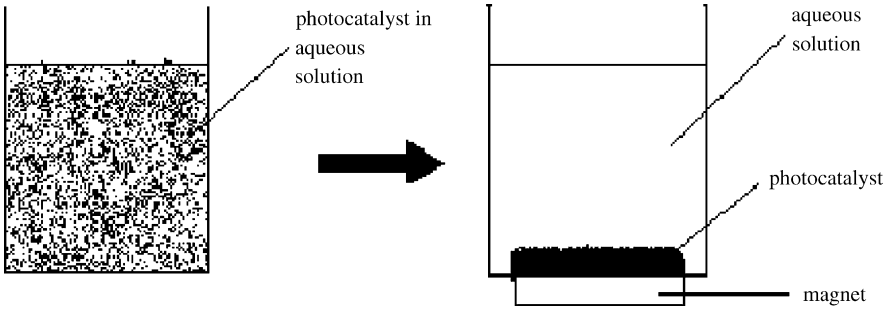

Scheme 1. Separation of photocatalyst by a magnet.

tocatalyst can be separated much more easily compared to the traditional photocatalysts after its use in suspension systems. Importantly, the composite photocatalysts can be re-dispersed into aqueous solution by ultrasonic vibrating after removing the magnet.

3. Results and discussion

3.1. Structures and morphologies

XRD patterns of prepared samples are presented in Fig. 1. Fig. 1(a) shows XRD pattern of the magnetic nanoparticles, presenting the characteristic peaks signed by F (30.4°, 35.7°, 53.8°, 43.4°, 57.4°, 63.0°) of cubic spinel structure. The iron oxide can be present as magnetite and maghemite because part of Fe_3O_4 particles may be oxidized to γ-Fe_2O_3. It can also be seen from Fig. 1(b) and (c) that the magnetic particles maintain cubic spinel structure in MAC and TMAC samples. This implies that the magnetic properties of the magnetic particles are basically invariable.

The TiO_2 deposited has an anatase structure in TMAC sample, determined from XRD pattern in Fig. 1(c) where the peaks signed by A (25.4°, 38.0°, 48.0°, 54.7°) are the characteristic peaks of anatase structural TiO_2. The peaks can be observed more distinctly from the XRD pattern of pure titania shown in Fig. 1(d). In general, the full width at half maximum of XRD peak corresponds to the crystal size. When the width was broader, the crystallites exhibited smaller size. Broad diffraction peak originating from (1 0 1) plane ($2\theta = 25.4°$) was due to its small crystallite size of TiO_2 sol particles.

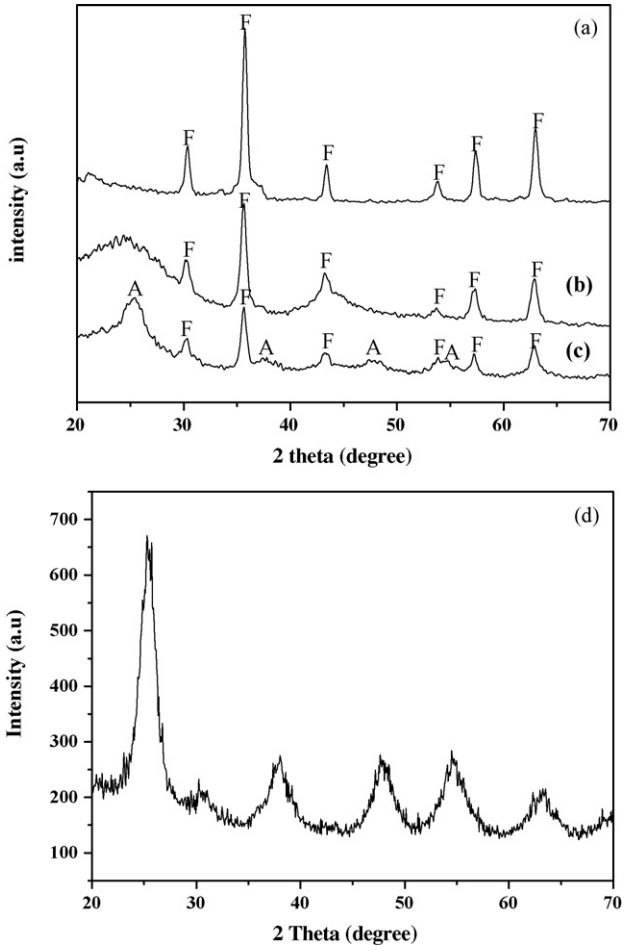

Fig. 1. XRD patterns of prepared samples: (a) Fe_3O_4; (b) magnetic activated carbon; (c) TiO_2-coated magnetic activated carbon; (d) pure titania.

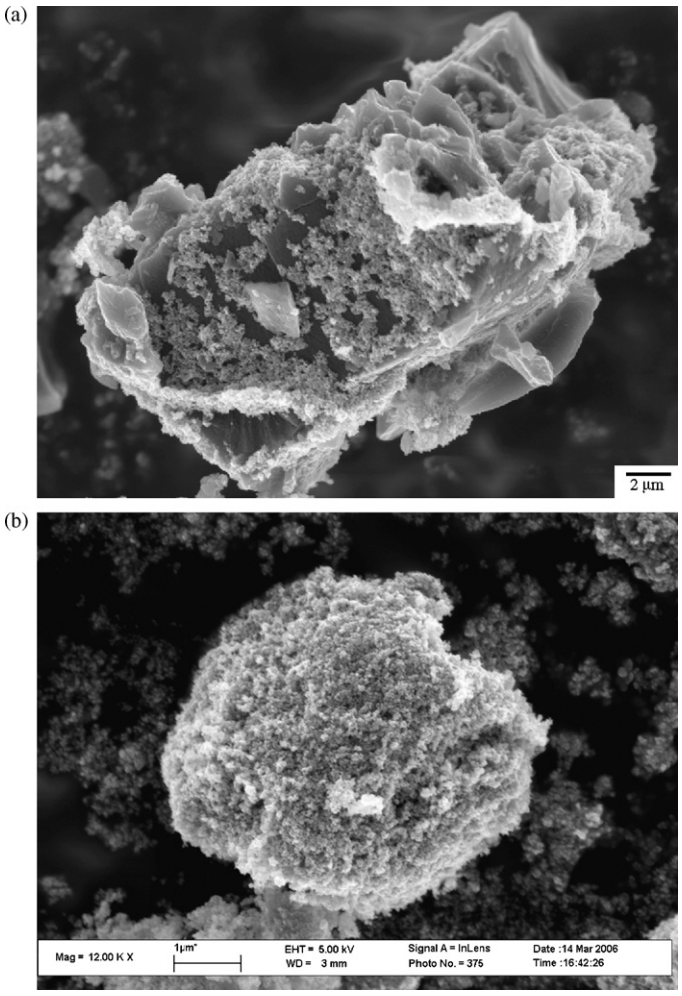

Fig. 2. SEM micrographs of (a) magnetic activated carbon and (b) TiO_2-coated magnetic activated carbon.

The mean size of the single crystallite can also be determined from full-width at half-maxima of corresponding X-ray diffraction peaks by using Scherrer's formula $D = (K\lambda)/(\beta \cos\theta)$, [20] where λ is the wavelength of the X-ray radiation (λ = 0.15418), K the Scherrer constant ($K = 0.9$), θ the characteristic X-ray radiation ($\theta = 12.7°$) and β is the full-width-at-half-maximum of the (1 0 1) plane. The estimated nanocrystallite size of TiO_2 sol sample was 4.8 nm.

It is believed that the photocatalytic effects of TiO_2 are mainly due to anatase structural TiO_2. In the previous reported magnetic iron oxide/titanium dioxide photocatalysts, some structural characteristics formed during calcination at high temperature have been considered to lead a decrease in the photoactivity [21–24]. For example, it had been found that the presence of the iron oxide could cause anatase to rutile phase transformation of the coating [24,25], or the possible formation of a mixed iron/titanium oxide (pseudobrookite, Fe_2TiO_5) [26,27]. Furthermore, the calcination at high temperature would also lead to the aggregation and enlargement of TiO_2 nanoparticles, which involve decrease of surface area and losses of species such as hydroxyl and adsorbed water that dominate the surface chemistry and adsorption activity of titania [28]. Our preparation and coating process at low temperature avoided or reduced the structural changes of TiO_2 sol when it deposited onto MAC as demonstrated from XRD patterns.

The results also show that the ACs did not influence the crystal structure of TiO_2 and iron oxide during our preparation. In obtained composites, all four components (AC, anatase TiO_2, cubic spinel

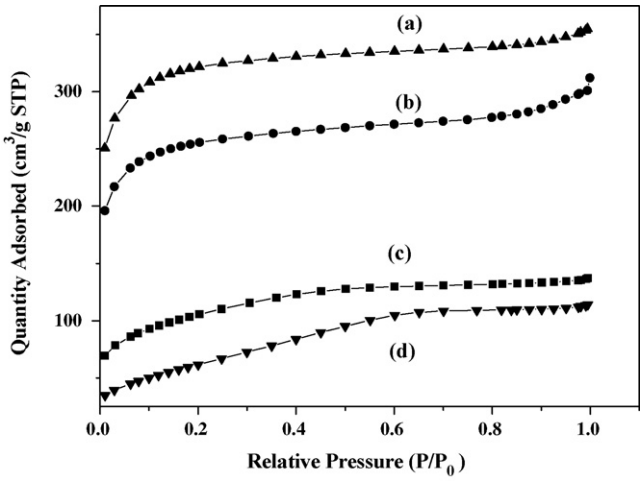

Fig. 3. BET isotherm plot of (a) AC; (b) MAC; (c) TMAC; (d) titania.

magnetite or maghemite) exist and there is no new compound has been formed.

After in sequence deposition of Fe_3O_4 and TiO_2, the surface of AC has been coated by TiO_2 nanoparticles. Although the puckered morphology of AC has been smoothed to a certain extent, the mounted titania layer is still porous as seen from SEM images (Fig. 2).

3.2. Surface area and pore volume measurements

BET isotherm plots of MAC and TMAC are shown in Fig. 3. Table 1 shows the results from surface area measurements of the different samples. As it can be seen, the higher AC contents of the catalysts the larger surface area. In addition, the pore diameter distributions of different samples were shown in Fig. 4. The pore diameter centred at 3.5 nm, 3.9 nm, 3.9 and 15.2 nm, 3.4 and 7.4 nm for pure titania, AC, MAC and TMAC, respectively. The pores centred at 15.2 nm and 7.4 nm may be formed by the magnetic and TiO_2 particles agglomerate on the AC particles.

Table 1
Surface area measurement of the different samples

Sample	AC content (%)	BET specific surface ($m^2\ g^{-1}$)	Pore volume ($cm^3\ g^{-1}$)
AC	100	1093.07	0.54
MAC	83	870.50	0.46
TMAC	28	373.56	0.21

If assuming all BET surface area and pore volume are contributed from activated carbon (AC), the normalized BET surface area S' ($S' = S/w$, where S is the BET surface area of sample and w is the weight percentage of AC in sample) are 1093.07 $m^2\ g^{-1}$ for neat AC, 1048.8 $m^2\ g^{-1}$ for MAC and 1334.1 $m^2\ g^{-1}$ for TMAC, respectively. The normalized pore volume V' ($V' = V/w$, where V is the pore volume of sample and w is the weight percentage of AC in sample) should be 0.54 $cm^3\ g^{-1}$ for neat AC, 0.55 $cm^3\ g^{-1}$ for MAC and 0.75 $cm^3\ g^{-1}$ for TMAC, respectively. Compared to the neat AC, the value of S' of MAC decreased and value of V' kept unchanged basically. This result seems to indicate that magnetic particles deposited mostly on the surface of AC, but some of them blocked up the entrance of the pores. Although Fe_3O_4 particles deposited on AC surface formed new BET surface area, this cannot compensate the decrease in AC surface area due to the decreasing of micropores. However, subsequent coating of MAC by TiO_2 nanoparticles largely increased normalized BET surface area S' (enhanced 241.03 $m^2\ g^{-1}$ compared to MAC). This increasing is consistent with following facts: (1) TiO_2 nanoparticles have larger adsorption ability than Fe_3O_4 nanoparticles. (2) A more porous coating layer formed when TiO_2 nanoparticles deposited onto the MAC particles as confirmed from SEM imaging (Fig. 5) and informed by normalized pore volume V' (enhanced 0.2 $cm^3\ g^{-1}$ compared to MAC). With above considerations, we should keep in mind that AC provide most important adsorption ability in TMAC catalyst, i.e. less AC content, smaller surface area and pore volume.

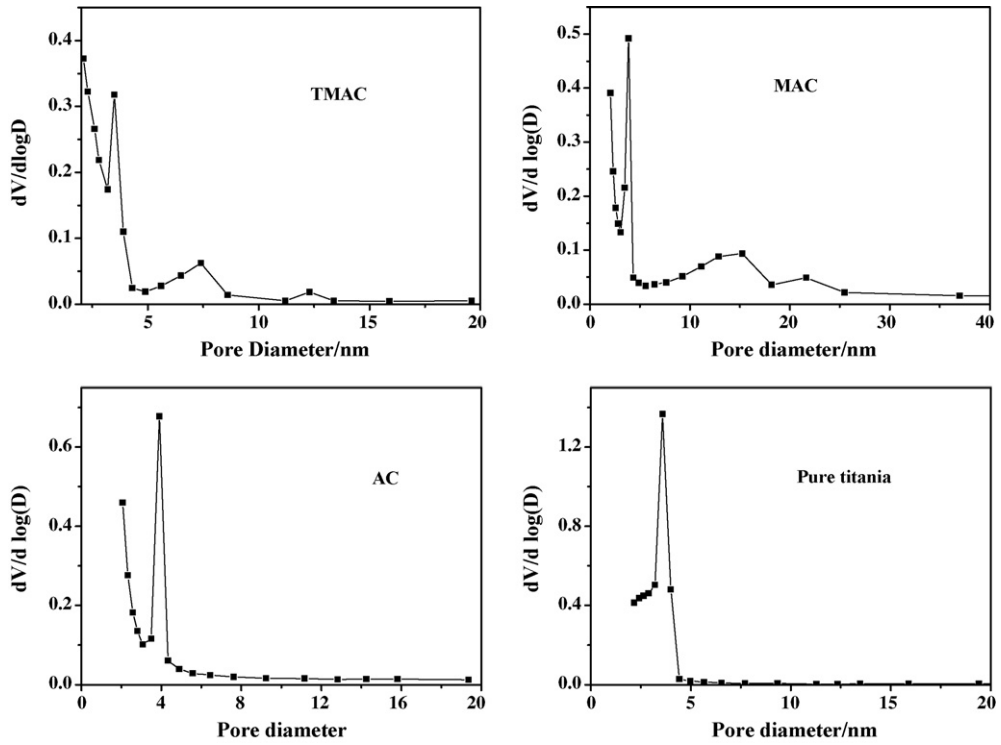

Fig. 4. Pore diameter distribution of different samples.

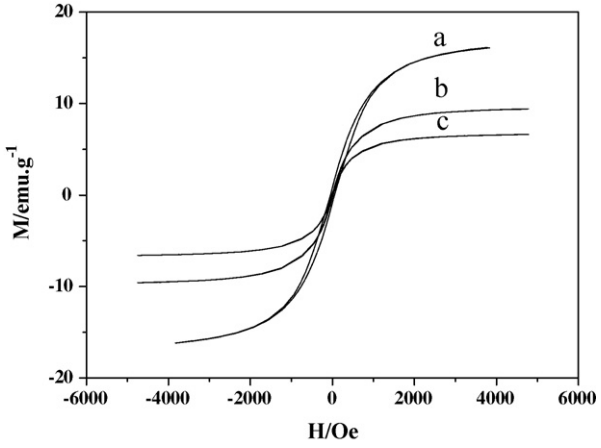

Fig. 5. Magnetization vs. applied magnetic field for the different samples: (a) Fe_3O_4/4; (b) MAC; (c) TMAC.

3.3. Magnetic properties

The magnetic properties of the Fe_3O_4 (F), MAC and TMAC samples were measured by VSM, as shown in Fig. 6. The magnetic parameters such as saturation magnetization M_s, coercivity H_c and remanent magnetization M_r were given in Table 2. The decrease of saturation magnetization M_s in the order of Fe_3O_4, MAC, and TMAC is consistent with their Fe_3O_4 content in unit weight sample. The low values of H_c and M_r which are close to zero indicate that the prepared samples exhibited superparamagnetic behaviors at room temperature [29]. The superparamagnetic behaviors of the prepared TMAC make the photocatalyst can be separated more easily by a magnet or an applied magnetic field. In the meantime, the very low remanent magnetization largely reduced the aggregation of catalyst after it was separated by applied magnetic field from original reaction solution, so the photocatalyst can be easily re-dispersed in a solution for re-use.

3.4. Photocatalytic activity

Photocatalytic properties of thus prepared samples were tested for the photocatalytic oxidation of phenol in aqueous solution and the result was showed in Fig. 7. The direct photolysis of phenol without photocatalyst was also investigated (not shown here). And the value can be neglected with less than 5% of conversion within 6 h

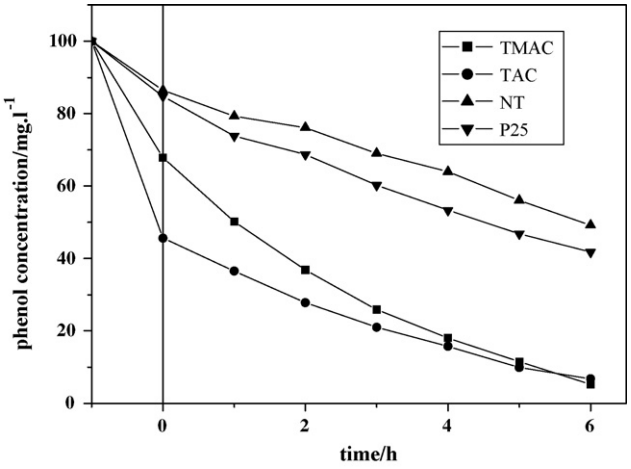

Fig. 6. Kinetics of phenol disappearance for different samples. The vertical line at time = 0 separates the dark period from the UV-irradiated process.

Table 2
Magnetic properties of the different samples

Samples	Coercivity H_c (Oe)	Remanent magnetization M_r (emu/g)	Saturation magnetization M_s (emu/g)
F	50.245	4.26	80.79
MAC	11.757	0.20	9.50
TMAC	12.552	0.17	6.45

of UV-irradiation. It can be seen from the figure that TMAC exhibits the best photocatalytic activity among the four photocatalysts, 96% of the total phenol was degraded after 6 h irradiation by UV lamp. The percentage of degraded phenol is 1.8 times higher than that of neat titania (NT) synthesized by the same method. The apparent rate constant has been chosen as the basic kinetic parameter for the different photocatalysts, since it enables one to determine a photocatalytic activity independent of the previous adsorption period in the dark and the concentration of phenol remaining in the solution. The apparent first order kinetic equation $\ln(c_0/c) = k_{app}t$ was used to fit experimental data in Fig. 6, where k_{app} is apparent rate constant, c is the solution-phase concentration of phenol, and c_0 is the initial concentration at $t = 0$ [9]. The variations in $\ln(c_0/c)$ as a function of irradiation time are given in Fig. 7. It gives apparent rate constants k_{app} as 0.08544 h^{-1}, 0.11694 h^{-1}, 0.29523 h^{-1} and 0.37316 h^{-1} for NT, P25, TAC, and TMAC, respectively. The depositing of TiO_2 onto AC or MAC obviously creates an increase of the rate constant by a factor of 3.5 and 4.4 compared to the single phase titania, respectively.

The enhanced photoactivity of TMAC can be attributed to the synergy effect between titania and AC. AC which have strong adsorbent activity can concentrate the contaminated substrate to the titania, then the substrate can be degraded faster on the photo-irradiated titania. The result is in agreement with other investigators [9–12]. On the other hand, the magnetic particles (either Fe_3O_4 or γ-Fe_2O_3) close to the titania can attract photo-induced electrons and reduce the rate of electron-hole recombination, because they both have lower lying conduction band compared to titania.

3.5. The desorption of phenol which adsorbed on the photocatalyst

It was attempted to determine the quantity of phenol remaining present on the solid. Blank preliminary tests performed on the

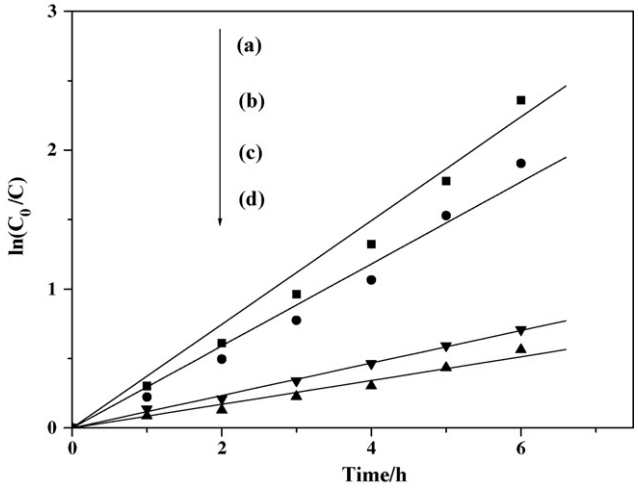

Fig. 7. Variations in $\ln(c_0/c)$ as a function of irradiation time and linear fits of them: (a) TMAC; (b) TAC; (c) P25; (d) NT.

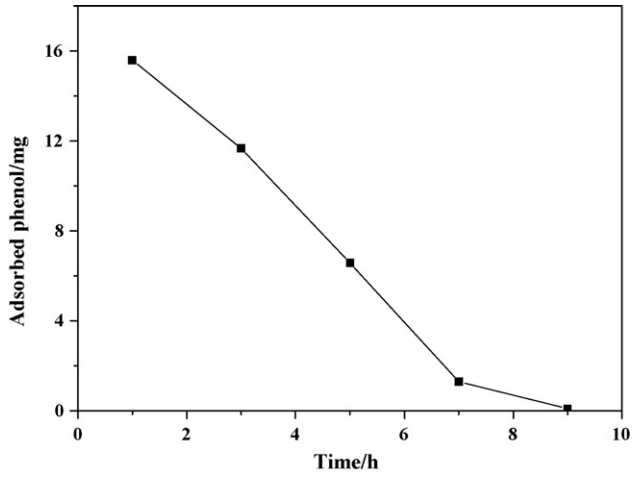

Fig. 8. Concentration of phenol extracted from the catalyst after being exposed to UV light for different times.

photocatalyst have shown that phenol could be extracted from AC with efficiency higher than 95%. The solid phase was therefore filtered and phenol was extracted in 20% acetonitrile solution under sonication for 30 min. It can be seen from Fig. 8 that the quantity of adsorbed phenol on the catalyst decreased as the irradiation time passed. A quantity of 2.12 mg of phenol could be extracted from the solid after 6 h of UV-irradiation when all the phenol had nearly disappeared from the solution. The quantity of phenol remaining adsorbed on the solid determined after extraction in acetonitrile reduced to nearly zero when the irradiation time increased to 9 h. Because the AC has no photo-activity, this figure clearly illustrates that molecules of phenol that have been adsorbed and accumulated on the AC during the 1 h adsorption and process of photocatalytic degradation are able to be transferred to titania where they are decomposed under irradiation.

4. Conclusions

We have illustrated a procedure for successfully fabricating magnetic activated carbon through the adsorption of iron oxide magnetic nanoparticles inside the pores and on the surface of a commercial activated carbon. This method suggests a simple route for the synthesis of magnetically separable activated carbons. Then the anatase titania particles prepared at low temperature (75 °C at most) were deposited onto the magnetic activated carbons. The titania-coated magnetic activated carbon (TMAC) thus prepared shows super-magnetic properties and can be separated easily by an external magnetic field. It can also be re-dispersed into aqueous solution by ultrasonic vibrating after removing the external magnetic field. The experiment results also suggest that the photocatalytic activity of TMAC was much higher than other three photocatalysts (Degussa P25, titania-coated activated carbon and neat titania synthesized by the same method).

Acknowledgements

This work was supported by the National Natural Science Foundation of China (No. 60121101) and Hi-Tech Research and Development Program (863 Program) of China (No. 2002AA302304). We are also very grateful to Prof. Zhang Yu and Dr. Liu Ji-wei in Southeast University for their help in VSM experiments.

References

[1] M. Pera-Titus, V. Garcıia-Molina, M. Banos, J. Gimenez, S. Esplugas, Degradation of chlorophenols by means of advanced oxidation processes, Appl. Catal. B 47 (2004) 219–256.
[2] D. Ollis, Contaminant degradation in water, heterogeneous photocatalysis degrades halogenated hydrocarbon contaminants, Environ. Sci. Technol. 19 (1985) 480–484.
[3] A. Mills, S. Hunte, An overview of semiconductor photocatalysis, J. Photochem. Photobiol. A 108 (1997) 1–35.
[4] M.R. Hoffmann, S.T. Martin, W.Y. Choi, Environmental applications of semiconductor photocatalysis, Chem. Rev. 95 (1995) 69–96.
[5] A. Fujishima, T.N. Rao, D.A. Tryk, Titanium dioxide photocatalysis, J. Photochem. Photobiol. C 1 (2000) 1–21.
[6] M.A. Fox, M.T. Dulay, Heterogeneous photocatalysis, Chem. Rev. 93 (1993) 341–357.
[7] R.L. Pozzo, M. Baltanas, A. Cassano, Supported titanium oxide as photocatalyst in water decontamination: state of the art, Catal. Today 39 (1997) 219–231.
[8] R. Matthews, Purification of water with near-UV illuminated suspensions of titanium dioxide, Water Res. 24 (1990) 653–660.
[9] J. Matos, J. Laine, J.M. Herrmann, Synergy effect in the photocatalytic degradation of phenol on a suspended mixture of titania and activated carbon, Appl. Catal. B 18 (1998) 281–291.
[10] B. Tryba, A.W. Morawski, M. Inagaki, Application of TiO_2-mounted activated carbon to the removal of phenol from water, Appl. Catal. B 41 (2003) 427–433.
[11] M. Toyoda, Y. Nanbu, T. Kito, M. Hirano, M. Inagaki, Preparation and performance of anatase-loaded porous carbons for water purification, Desalination 159 (2003) 273–282.
[12] E. Carpio, P. Zuniga, S. Ponce, J. Solis, J. Rodriguez, W. Estrada, Photocatalytic degradation of phenol using TiO_2 nanocrystals supported on activated carbon, J. Mol. Catal. A 228 (2005) 293–298.
[13] D. Beydoun, R. Amal, Novel photocatalyst: titania-coated magnetite: activity and photodissolution, J. Phys. Chem. B 104 (2000) 4387–4396.
[14] Y.S. Chung, S.B. Park, D.W. Kang, Magnetically separable titania-coated nickel ferrite photocatalyst, Mater. Chem. Phys. 86 (2004) 375–381.
[15] F. Chen, Y.D. Xie, J.C. Zhao, G.X. Lu, Photocatalytic degradation of dyes on a magnetically separated photocatalyst under visible and UV irradiation, Chemosphere 44 (2001) 1159–1168.
[16] S. Rana, J. Rawat, R.D.K. Misra, Anti-microbial active composite nanoparticles with magnetic core and photocatalytic shell: TiO_2–$NiFe_2O_4$ biomaterial system, Acta Biomaterialia 1 (2005) 691–703.
[17] S. Rana, R.S. Srivastava, M.M. Sorensson, R.D.K. Misra, Synthesis and characterization of nanoparticles with magnetic core and photocatalytic shell anatase TiO_2–$NiFe_2O_4$ system, Mater. Sci. Eng. B 119 (2005) 144–151.
[18] J. Rawat, S. Rana, R. Srivastava, R.D.K. Misra, Antimicrobial activity of composite nanoparticles consisting of titania photocatalytic shell and nickel ferrite magnetic core, Mater. Sci. Eng. C 27 (2007) 540–545.
[19] B.K. Sunkara, R.D.K. Misra, Enhanced antibactericidal function of W^{4+}-doped titania-coated nickel ferrite composite nanoparticles. A biomaterial system, Acta Biomaterialia 4 (2008) 273–283.
[20] Y.B. Xie, C.W. Yuan, Visible-light responsive cerium ion modified titania sol and nanocrystallites for X-3B dye degradation, Appl. Catal. B 46 (2003) 251–259.
[21] J.A. Navio, M. Macias, M. Gonzalez-Catalan, A. Justo, Bulk and surface characterization of powder iron-doped titania photocatalysts, J. Mater. Sci. 27 (1992) 3036–3042.
[22] R.I. Bickley, T.L. Gonzalez-Carreno, R.J. Palmisano, D. Tilley, J. Williams, Relative proportions of rutile and pseudo-brookite phases in the Fe(III)–TiO_2 system at elevated temperature, Mater. Chem. Phys. 51 (1997) 47–53.
[23] A. Milis, J. Peral, X. Domenech, Heterogeneous photocatalytic oxidation of nitrite over iron-doped TiO_2 samples, J. Mol. Catal. 87 (1994) 67–74.
[24] M.I. Litter, J.A. Navio, Comparison of the photocatalytic efficiency of TiO_2, iron oxides and mixed Ti(IV)–Fe(III) oxides, J. Photochem. Photobiol. A 84 (1994) 183–193.
[25] R.P. Madhusudhan, B. Viswanathan, P.P. Viswanath, Strong metal support interaction state in the Fe/TiO_2 system—an XPS study, J. Mater. Sci. 30 (1995) 4980–4985.
[26] J. Yuan, S. Tsujikawa, Photo-effect of sol–gel derived TiO_2 coating on carbon steel in alkaline solution, Zairyo-to-Kankyo 44 (1995) 534–542.
[27] J. Huang, T. Konishi, T. Shinohara, S. Tsujikawa, Effects of interfacial iron oxides on corrosion protection of carbon steel by TiO_2 coating under illumination, Zairyo-to-Kankyo 47 (1997) 651–661.
[28] R. Howe, M. Gratzel, EPR study of hydrated anatase under UV irradiation, J. Phys. Chem. 91 (1987) 3906–3909.
[29] Q.A. Pankhurst, J. Connolly, S.K. Jones, J. Dobson, Applications of magnetic nanoparticles in biomedicine, J. Phys. D 36 (2003) R167–R181.